Supplemental Information

EXTENDED EXPERIMENTAL PROCEDURES

Antibodies

The following primary antibodies were used in immunostaining: anti-GFP (Abcam ab290), anti-LaminA/C (SantaCruz sc-7292), anti-LaminB (SantaCruz sc-6216), anti-LaminB1 (Abcam ab16048), anti-LaminB2 (Abcam ab8983), anti-α-Tubulin (Sigma-Aldrich T5168), anti-Myc tag (Abcam ab9132), anti-PRR14 76-90 (Sigma-Aldrich SAB1102100), anti-PRR14 306-320 (Sigma-Aldrich SAB1102101), anti-LBR (Abcam ab122919).

siRNA sequences. PRR14 siRNA sequences (Dharmacon, ThermoScientific): #1 5'-CAACAAGAATTACCAATCA, #2 5'-GCTAGAAGATGTCATGGCT, #3 5'-GAGGATAGTTCGCCAGCCA, #4 5'-GGACTGCCTCGACCAATCA. Lamin A/C siRNA sequences: 5'-CAGGCAGTCTGCTGAGAGGAA, 5'-CCCACCAAAGTTCACCCTGAA, 5'-AACTGGACTTCCAGAAGAACA, 5'-CCAGGAGCTTCTGGACATCAA. Lamin B1 siRNA sequences: 5'-AACGCGCTTGGTAGAGGTGGA, 5'-CAGGGAGAGGAGGTTGCTCAA, 5'-CCCGAGCATCCTCAAGTCGTA, 5'-CTGGCGAAGATGTGAAGGTTA. Lamin B2 siRNA sequences: 5'-CAGCGCCAGGTTAACGCTGAA, 5'-TCGGCAATAGCTCACCGTTTA, 5'-CACGCGGCAGTTCTTTGTTAA, 5'-CGCCTACAAGTTCACGCCCAA. LBR siRNA sequences: 5'-TAAGGTAGCTTTAGCAATTAA, 5'-TAGCAATTAAATTCTAGTGAA, 5'-AGCGTTGTTGACGACCATGGA, 5'-CAGCGTGTGCCCTACCGTATA, 5'-CAGGCCGACATTAAGGAAGCA. HP1 siRNA SMARTpools (Dharmacon, ThermoScientific): CBX1 (HP1beta) M-009716, CBX3 (HP1gamma) M-010033, and CBX5 (HP1alpha) M-004296. SiControl, control siRNA (QIAGEN): AllStars Negative Control siRNA SI03650318.

Image analysis and quantitation

Image analysis was performed using Nikon EZ-C1 v3.8 (Nikon Instruments, Inc., Melville, NY) and MetaXpress v.3.1 software (MDS Analytical Technologies, Sunnyvale, CA). For Figures 1C and S4 the line profile tool was used. For Figures 2B and 2C, nuclear pixel-to-pixel channel overlap was quantitated for GFP-PRR14 (green) and mRFP-HP1a (red) (panel 2B), and PRR14 N-GFP 1-135 (green) and anti-H3K9me3 (red) (panel 2C). For these two panels multiple cells were analyzed (n = 15), and the results are presented graphically in the respective panels. For Figure 2D, channel overlap for nuclear PRR14 N-GFP 1-135 and two substituted forms (green) were each compared to Hoechst (blue). Multiple cells were analyzed (n = 15) for each comparison, and highly significant differences ($p < 0.00001$) between wt and substituted proteins were observed as presented graphically in panel 2D. For Figure 2E, the effect of PRR14 siRNA knockdown on peripheral H3K9me3 chromatin was measured by comparing H3K9me3 staining (green) with Lamin A/C staining (red). To quantitate loss of H3K9me3 at the nuclear periphery, a mask of the peripheral nuclear region was first created using the red channel. The fraction of the green signal within the peripheral region could then be compared to the total green signal intensity. Individual cells that had been treated with either control siRNA or PRR14 siRNA were compared (also see Figure S4). Multiple images were analyzed for each treatment (n = 25), and differences in H3K9me3 distribution between control and PRR14 siRNA-treated cells were highly significant (p-value < 0.00001) (Figure 2E). For Figure 2F, the effects on PRR14 localization after control, Lamin A/C, Lamin B1 and Lamin B2 siRNA knockdown were determined by comparing the PRR14 N-GFP signal (green) and Lamin B signal (red) channels (n = 16 for each treatment). Highly significant differences (p-value < 0.00001) between the control and Lamin A/C siRNA knockdowns were observed, as presented graphically in Figure 2F. For Figure S2D, channel overlap for nuclear PRR14 N-GFP 1-135 (green) to Hoechst (blue) was compared in the control and HP1 knockdown samples. Multiple cells were analyzed (n = 20) for each sample, and highly significant differences ($p < 0.00001$) between control and HP1 knockdown sample were detected. For Figure S2E, the effect of LBR, Lamin A/C and PRR14 siRNA knockdowns on peripheral H3K9me3 chromatin was measured similarly as described in Figure 2E, using Lamin B signal (red) to create a peripheral region mask. Multiple images were analyzed for each treatment (n = 20), and differences in H3K9me3 distribution between siRNA control and siRNA target samples were $*p = 0.0188$ and $**p < 0.00001$, respectively as shown on figure S2E.

SUPPLEMENTAL MOVIE LEGEND

Movie S1. Binding of PRR14 to mitotic chromatin at the onset of anaphase.
Left panel, DNA (Hoechst staining). Middle panel, N-GFP-tagged PRR14 protein. Right panel, merge. HeLa cells stably expressing N-GFP-tagged PRR14 protein were synchronized using a double thymidine block. The metaphase-anaphase-telophase transition is shown.

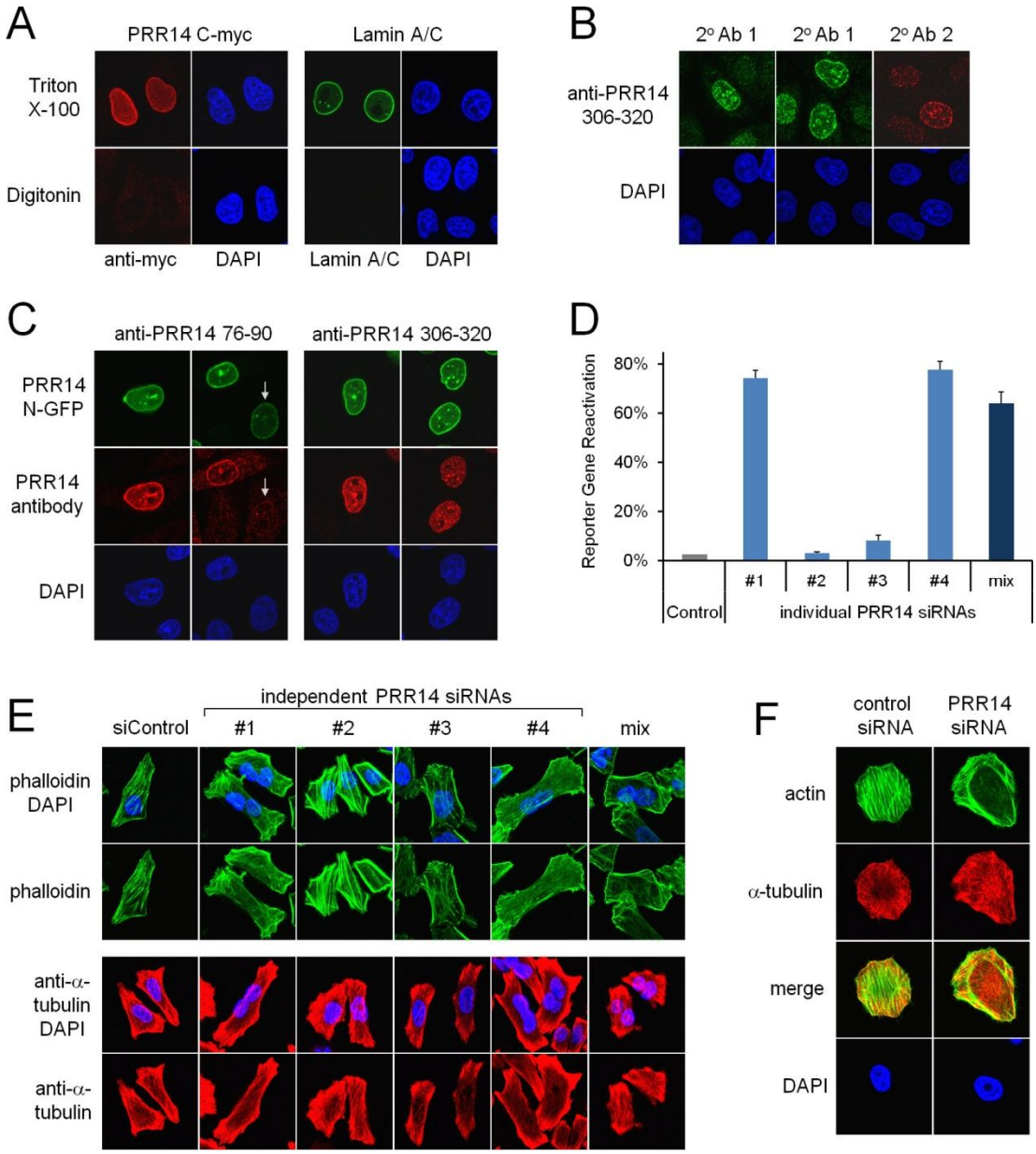

Figure S1. Detection of native PRR14 in HeLa cells and role in nuclear lamina structure, related to Figure 1.

(A) HeLa cells were transfected with myc-tagged PRR14, and cells were permeabilized using differential conditions that allow antibodies to penetrate either the plasma membrane only (digitonin), or both the plasma and nuclear membranes (Triton-X 100). PRR14 protein and Lamin A/C were detected only after Triton X-100 treatment, indicating that the tagged PRR14 was concentrated at the inner nuclear periphery. Control experiments confirmed conditional access to cytoplasmic components or the nuclear lamina (data not shown).

(B) Native PRR14 was detected using a peptide antibody corresponding to positions 306-320. Two different secondary antibodies were used to confirm that staining at the nuclear periphery was specific.

(C) The efficiencies of two PRR14 antibodies targeting amino acids 76-90 and 306-320 were compared using transfected N-terminal GFP-tagged PRR14. Peptide antibody to positions 76-90 detected transfected PRR14 at the periphery, while the 306-320 antibody favored detection of nucleoplasmic PRR14. Transfected GFP-tagged PRR14 reacted weakly with both antibodies. For example, a cell with moderate levels of GFP-tagged PRR14 expression shows no significant staining with the 76-90 anti-PRR14 antibody (arrow). We conclude that the inability to detect native PRR14 with the 76-90 antibody is due to weak reactivity. We also conclude that the epitope for the 306-320 antibody can be blocked in some cells by nuclear lamina association.

(D) GFP reactivation assay is shown (Poleshko et al., 2010). Treatment with PRR14 siRNAs #1 and #4 resulted in reactivation of an epigenetically silent GFP reporter gene.

(E) Treatment with independent PRR14 siRNAs (#1 and #4), as well as a PRR14 siRNA mix caused detachment of the nucleus from the actin cytoskeleton in HeLa cells, as well as binucleation. SiRNA #3 produced a weaker, but reproducible effect. No significant effect on microtubules was detected. siControl, control non-targeting siRNA.

(F) Cells were treated with control or the PRR14 siRNA mix, and stained for actin and α-tubulin simultaneously.

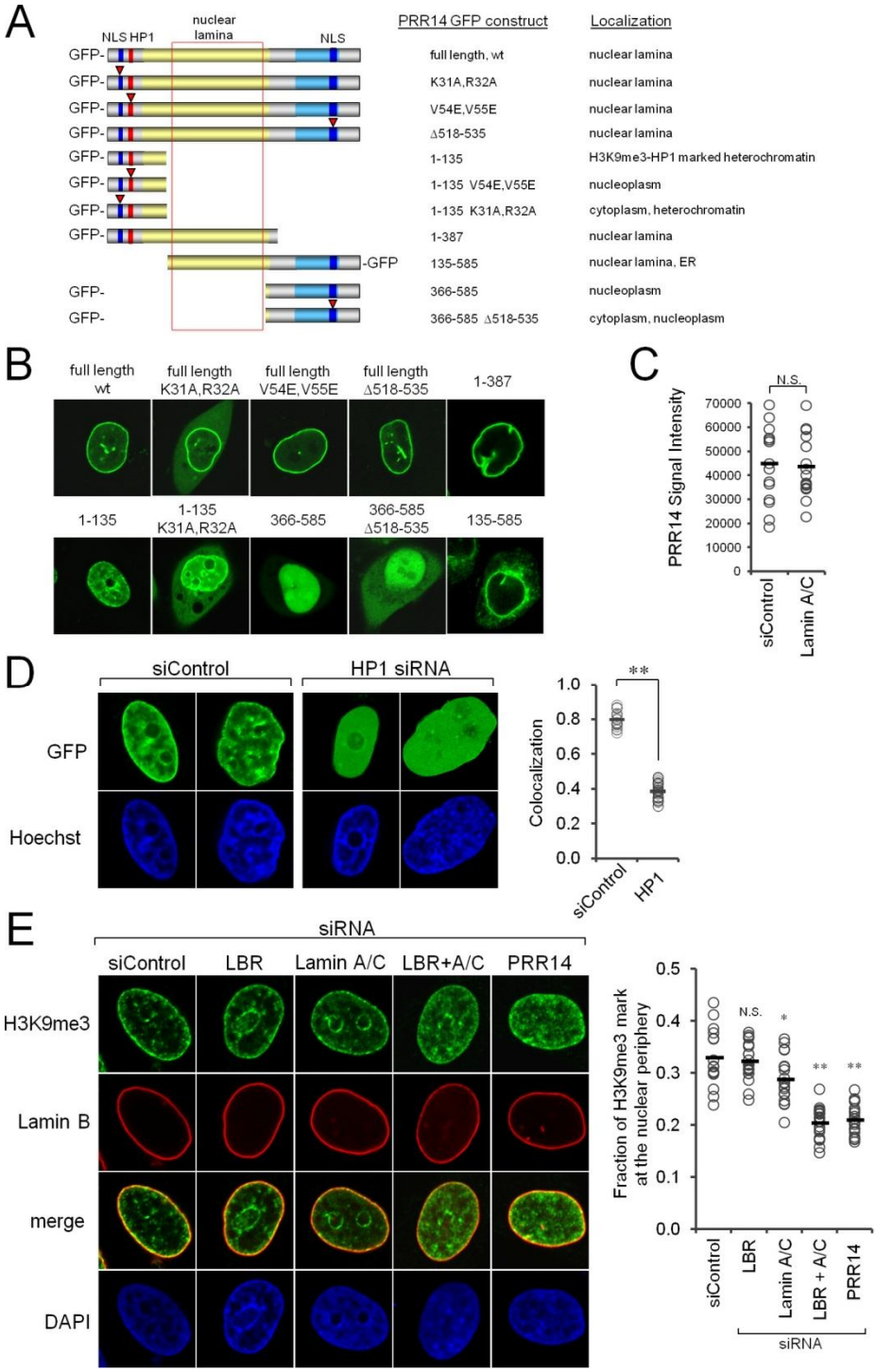

Figure S2. Mapping of PRR14 domains, subcellular localization, and effects of PRR14 knockdown on H3K9me3 heterochromatin, related to Figure 2.

(A) PRR14 map is shown (yellow, proline rich region; light blue, conserved region; red, HP1-binding motif; dark blue, NLSs). Substitutions and small deletions are indicated with red arrow heads.

(B) Confocal imaging of substituted and truncated GFP-tagged PRR14 proteins. Representative images are shown based on > 15 examples. PSORT analysis detected three potential NLSs at positions 30-36 in the N-terminal fragment, 357-363 in the central region (not shown), and 518-534 in the C-terminal fragment. Consistent with the NLS predictions, N-terminal (positions 1-135) and C-terminal fragments (positions 366-585) both localize to the nucleus. Site-specific mutagenesis of the candidate signals at positions 30-36 and 518-535 resulted in nuclear import defects of the respective fragments. In the context of the full length N-terminal GFP fusion, disruption of the candidate N-terminal NLS caused a partial nuclear import defect, while deletion of the C-terminal NLS had no significant effect. The N-terminal NLS substitution, a large fraction of cells showed cytoplasmic accumulation, while some cells showed nuclear accumulation consistent with nuclear entry of the NLS substituted protein during mitosis. The 1-387 and 135-585 fragments both showed nuclear lamina localization as well as internal tube-like structures similar to the wild type protein.

(C) Quantitation of total nuclear signal intensity of GFP-tagged PRR14 after knockdown of Lamin A/C using MetaXpress software. Statistical analysis indicates that Lamin A/C knockdown did not cause significant changes in total signal intensity, N.S., not significant (n = 15 for each sample).

(D) HeLa cells stably expressing the GFP-tagged PRR14 1-135 fragment were transfected with siRNAs targeting all three HP1 isoforms. Confocal imaging of live cells is shown. Dense chromatin regions were detected with Hoechst (blue). The results are expressed as the fraction of colocalizing green and blue signals in individual cells (n = 20). ** indicates a p-value < 0.00001 for differences between control and HP1 siRNA knockdown cells.

(E) Measurement of disassociation of H3K9me3-marked chromatin from nuclear perphiphery after siRNA-based knockdown of LBR, Lamin A/C, LBR plus Lamin A/C or PRR14. Experimental design and statistical analyses are as described in Figure 2E. Results of statistical analyses are indicated: N.S., not significant; *p = 0.018, **p < 0.00001 (n = 20 for each sample).

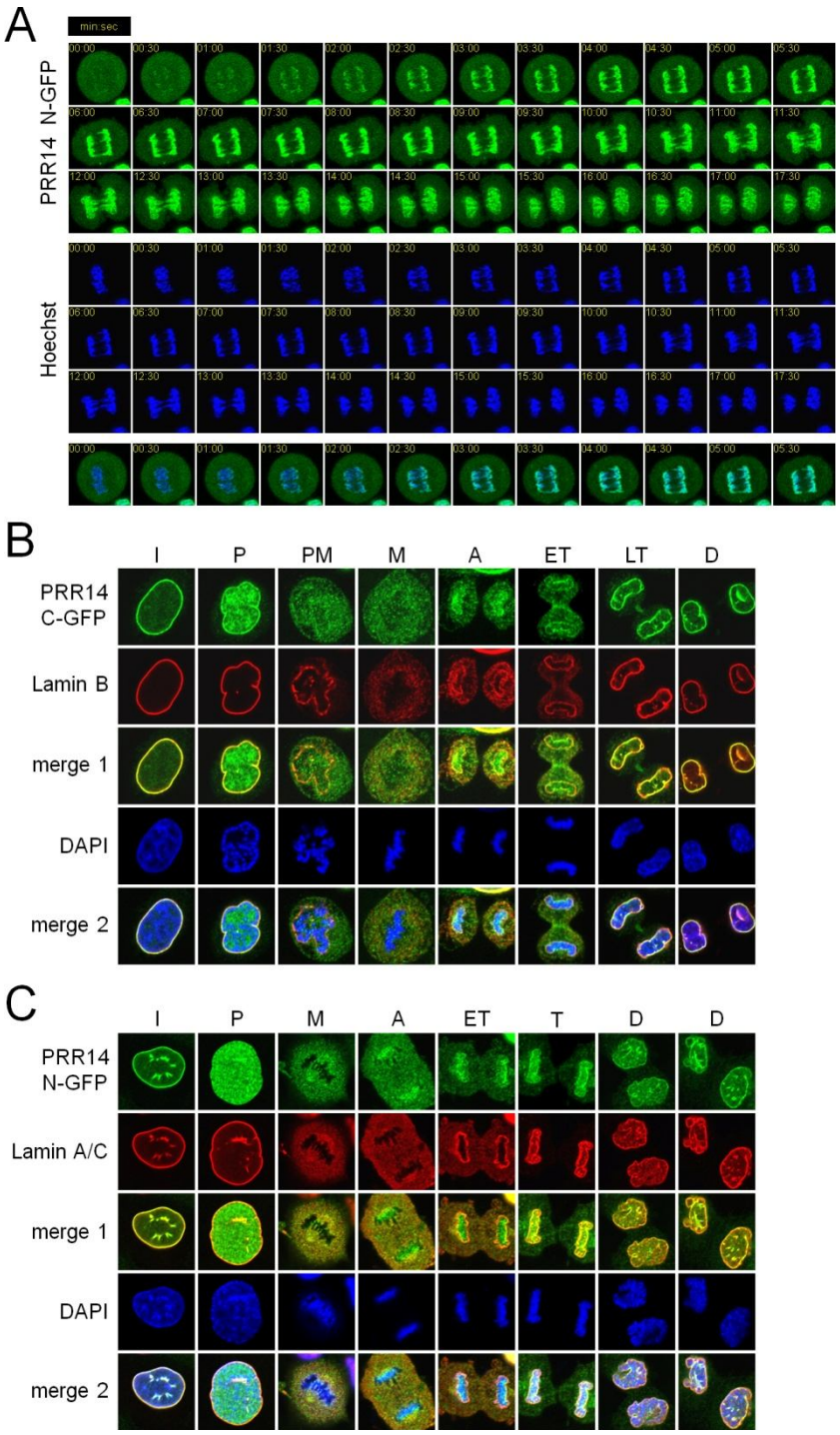

Figure S3. Confocal imaging of GFP-tagged PRR14 proteins during mitosis, related to Figure 3.

(A) Time lapse confocal imaging (thirty second intervals) of HeLa cells stably expressing N-terminal GFP-tagged PRR14. The metaphase to anaphase to telophase transitions are shown. GFP (top, green); DNA visualized with Hoechst (middle, blue). Merged images of the first 4 minutes of anaphase are shown (bottom).

(B) Mitotic behavior of C-terminal GFP-tagged PRR14, stably expressed in HeLa cells. The following abbreviations are used to indicate stages of mitosis: interphase, I; prophase, P; prometaphase, PM; metaphase, M; anaphase, A; early telophase, telophase, and late telophase, ET, T, LT; daughter cells, D.

(C) Mitotic behavior of N-terminal GFP-tagged PRR14, stably expressed in RPE1 cells. Methods and stage designations are as in panel B. The behavior of PRR14 is similar to that observed with N-terminal GFP-tagged PRR14 in HeLa cells (Figure 3A). In these experiments (panel B and C), the GFP signal was enhanced with anti-GFP antibody.

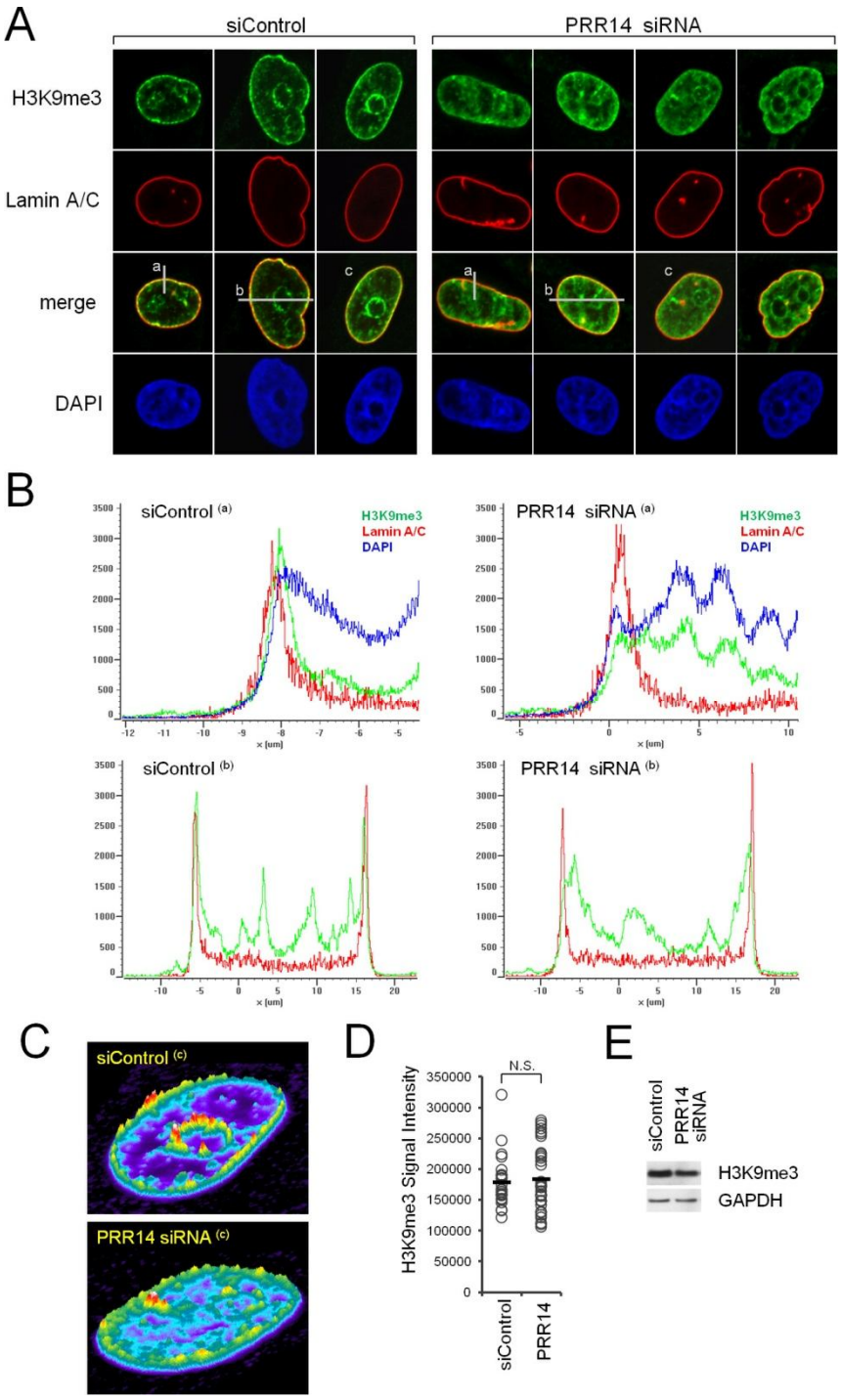

Figure S4. Image analysis of detachment of H3K9me3-marked chromatin from the nuclear lamina after PRR14 siRNA knockdown, related to Figure 2E.

(A) Shown are representative images of the experiment described in Figure 2E. HeLa cells were transfected with PRR14 siRNA and control siRNAs, and after 72 hrs, co-staining with anti-H3K9me3 (green) and Lamin A/C (red) antibodies was carried out. Confocal images are shown along with a merged image of the red and green channels.

(B) Line profile scans of signal intensity in the regions indicated in panel A were analyzed using Nikon EZ-C1 FreeViewer v3.3 software. Superscripts a and b correspond to scans generated from the indicate lines in panel A. Scans are consistent with detachment of H3K9me3 chromatin from the nuclear lamina after PRR14 knockdown.

(C) Three dimensional image profiles were generated using MetaXpress software. Superscript c corresponds to images in panel A. The profiles are consistent with detachment of H3K9me3 marked chromatin from the nuclear periphery after PRR14 knockdown.

(D) Quantitation of total nuclear signal intensity of H3K9me3 after knockdown of PRR14 using MetaXpress software. Statistical analysis indicates that PRR14 knockdown did not cause significant changes in total signal intensity (N.S., not significant).

(E) Western blot analysis of PRR14 siRNA knockdown is shown. No major changes in the total level of H3K9me3 histone mark were observed.

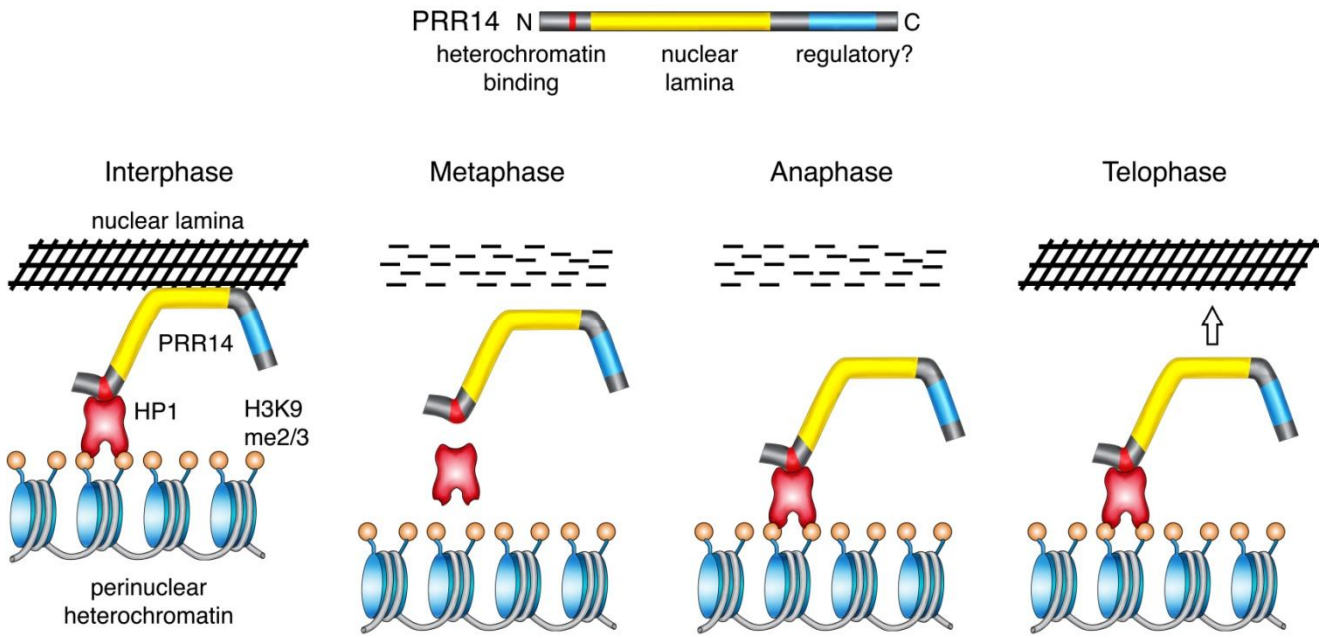

Figure S5. Proposed model for PRR14 function in tethering, and mitotic specification of HP1-H3K9me2/3-marked heterochromatin for attachment at the nuclear lamina, related to Figures 2 and 3.

Color coding of PRR14 regions is as described in Figure 2A. The model first depicts PRR14 tethering HP1-H3K9me3-marked heterochromatin to the nuclear lamina in interphase (left). The association of PRR14 with the nuclear lamina may be direct or indirect. In prophase and metaphase, the tether components disassemble to allow chromosome condensation. In anaphase, HP1 and PRR14 begin to rebind to chromosomes through the H3K9me2/3 mark, which is retained throughout mitosis. In mid- to late-telophase the pre-assembled PRR14-HP1-H3K9me3 heterochromatin complex reassociates with the formed nuclear lamina (arrow), thus reestablishing the tethered state.